Effect of Shielding and Drain Wire on Lightning-induced Currents in Rotorcraft Cables

Jaehyeon Jo, *Student Member, IEEE*, Yungon Kim, Donghyeon Kim, Hakjin Lee, and R. S. Myong, *Member, IEEE*

***Abstract*—A strong electromagnetic field can be induced by lightning strikes on an aircraft and cause serious disturbances in electronic equipment and cables inside the aircraft. In this study, the performance of a cable protection system consisting of shielding and drain wire in an indirect lightning environment was analyzed using tests and computational simulations. The cable bundle test was conducted according to RTCA DO-160 Section 22. The shielding and drain wire performance was quantitatively evaluated by monitoring the magnitude of the induced current generated in the cable bundle. First, it was generally found that shielding was more effective than drain wire for protecting cables from lightning. In the case of the drain wire, the drain wire with high electrical conductivity showed better performance. In addition, the protection performance of the shielding and drain wire was predicted by computational simulation using the software EMA3D. Finally, the performance of the shielding and drain wires on the inner cables of the EC-155B helicopter was analyzed using computational simulations.**

***Index Terms*—DO-160 Section 22, Cable bundle, Rotorcraft, Lightning Indirect Effect, Airworthiness Certification**

I. Introduction

AIRCRAFT experience various weather environments during flight, and among them, lightning strikes can seriously affect the safe operation of the aircraft. The extremely high temperatures and strong currents of lightning strikes can cause serious physical damage to aircraft structures and components such as fuel tanks. Moreover, lightning causes a strong electromagnetic field near the aircraft, which induces an electric current in the system of interconnecting cables and electric equipment. Lightning-induced currents in the cables can cause the avionics to malfunction and can lead to an unfortunate aircraft accident [1]-[6]. Therefore, the risk of aircraft damage or accidents is increased substantially by adverse weather conditions such as storms. Lightning strikes are mainly caused by atmospheric discharges in cumulonimbus clouds. According to statistical surveys of lightning-related aircraft incidents, aircraft are struck by lightning more than once a year [7], [8].

Recently, several cases of electronic equipment failures inside aircraft due to strong electromagnetic fields generated by lightning strikes have been reported. For instance, in October 2014, a United Airlines Boeing 787-824 N26906 departing from London, England, was struck by lightning. As a result, the power to 3 out of 5 HDDs (Heads Down Displays) located in the cockpit was shut down [9]. In addition, in May 2019, an Aeroflot Russian Airlines Sukhoi Superjet 100 airliner departed from Sheremetyevo, Russia, was struck by lightning shortly after takeoff, and made an emergency landing, resulting in 41 deaths due to fire [10].

To ensure safe flight in a lightning environment, the Federal Aviation Administration (FAA) and the European Aviation Safety Agency (EASA) have published certification guidelines [11]. In particular, the FAA commissioned SAE International to formulate the SAE Aerospace Recommended Practice (ARP) [12]. The procedure for demonstrating conformity to the indirect effect of lightning is included in AC 20 136C, established by the FAA [11].

In previous works lightning's indirect effects on cables have been studied using measurements in test facilities and computational analysis. Zhang *et al.* [13] predicted the magnitude of the current induced on a cable inside the aircraft using computational simulation and discussed the effect of shielding on cables. Parmantier *et al.* [14] investigated lightning indirect effects on shielded cable harness inside a rotorcraft using computational simulation. Lalonde *et al.* [15] conducted pin injection tests of aircraft cables in an indirect lightning environment. Huang *et al.* [16] and Wang *et al.* [17] conducted an indirect lightning test on a full-scale rotorcraft to measure the magnitude of the current induced on the cables. He *et al.* [18] and Filik *et al.* [19] investigated the cable test method included in the Radio Technical Commission for Aeronautics (RTCA) DO-160, a standard for the environmental testing of avionics hardware, and performed tests and computational simulations.

Shielding is one of the most effective ways of protecting cables against the high electromagnetic field caused by lightning strikes. The shielded wire can adequately protect the cable from lightning conditions and can reduce the magnitude of the current induced in the cable. For this reason, most previous studies have focused on the effect of shielding on lightning-induced currents in cables.

In the present study, a drain wire is considered as a cable protection system in addition to the well-known shielding. To this end, cable bundle tests and calculation simulations are performed to verify protection performance. To the author's best knowledge, very few studies have investigated the performance of a drain wire

This work was supported the National Research Foundation of Korea (NRF) Grant funded by the Ministry of Science, ICT & Future Planning (NRF-2017-R1A5A1015311) and the Korea Institute of Aviation Safety Technology (KIAST) Grant funded by the Ministry of Land, Infrastructure and Transport (21CHTR-C128889-05), South Korea. The authors thank the referees of this paper for their valuable comments. (*Corresponding author: R. S. Myong*)

Jaehyeon Jo, Yungon Kim, Donghyeon Kim, Hakjin Lee and Rho Shin Myong are with Gyeongsang National University, Jinju, Gyeongnam 52828, South Korea. Yungon Kim is currently with Aerospace EM Technology Center, Korea Testing Laboratory, Jinju, Gyeongnam 52852, South Korea. (E-mail: skrave08@gnu.ac.kr; rudtkd4573@gnu.ac.kr; kdh8712@gnu.ac.kr; hlee@gnu.ac.kr; myong@gnu.ac.kr).

using both the experimental and computational approaches. The time variation and the maximum magnitude of the current induced on the cables with and without the protection system were compared under various lightning conditions, in terms of waveforms and levels. A cable bundle test was conducted according to RTCA DO-160 Section 22, a certification guideline for aircraft internal electronic equipment and cables. In addition, electromagnetic analysis was performed using EMA3D software and the predicted results were compared with experimental data. Finally, to investigate the feasibility of the cable protection systems (shielding and drain wire) for reducing lightning-induced currents on the rotorcraft, the cable harness connecting the cockpit, engine, landing gear, and tail boom of an EC-155B civil helicopter was analyzed using computational simulations.

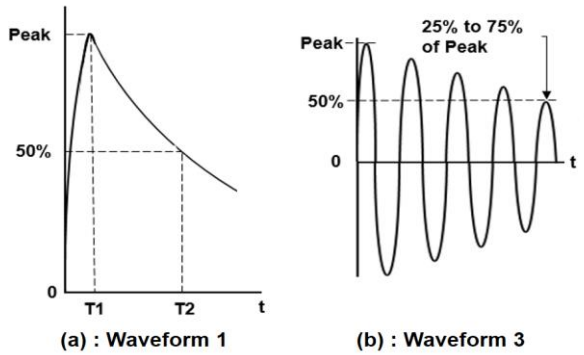

Fig. 1. Test waveforms 1 and 3 for the lightning indirect test.

II. CABLE BUNDLE TEST

RTCA DO-160 contains test regulations for electronic equipment and cables mounted on aircraft. In particular, Section 22 contains the test methods and procedures for the indirect effects of lightning on equipment to be evaluated [20].

Test waveforms 1 and 3 used in this study are shown in Fig. 1, which are generated by a transient generator and sent to the coupling transformer as source waveforms. The essential parameters of test waveform 1 are the time T1 at the maximum value and the time T2 at the halving after the maximum current value. The key property of test waveform 3 is that it has half the maximum current amplitude in the fifth from the period with the first maximum amplitude of the oscillating waveform. RTCA DO 160 Section 22 specifies that waveform 1 should be used for shielded situations, while waveforms 1 or 3 should be used for unshielded situations. Accordingly, test waveform 3 was chosen to simulate the unshielded/shielded situations on the aperture coupling [20]. Moreover, test waveform 1 was chosen to compare the performance of the drain wire for cable protection by increasing the cable numbers. In addition, test level 3, which assumes a lightning transient environment inside the cockpit, and test level 5, which assumes an extreme lightning environment in the rotorcraft, were applied.

A. Test Cable and Drain Wire

In this test, American Wire Gauge (AWG) 20 cable M5086/1-20 was used. The components and thickness of the cable and drain wire are shown in Fig. 2 and Table I, respectively. The thickness of the cable filler and the jacket were 0.1016 mm, and 0.1524 mm, respectively. The M5086/2-20 cable was treated with a 0.127 mm thick impregnated copper shield and was used to investigate the cable shielding performance. The drain wire was connected to the ground, as shown in Fig. 2. The drain wire used in this test was made of copper and aluminum to compare the cable protection performance in relation to electrical conductivity. The length of each cable and drain wire was selected to be 4 m.

TABLE I
MATERIAL AND THICKNESS OF CABLES AND DRAIN WIRE

	M5086 /1-20	M5086 /2-20	Drain Wire
Conductor	Tinned Copper (0.032mm)	Tinned Copper (0.032mm)	Copper /Aluminum (0.032mm)
Filler	PVC (0.1016mm)	PVC (0.1016mm)	-
Shield	-	Impregnated Braid (0.1270mm)	-
Jacket	Nylon (0.1524mm)	Nylon (0.1524mm)	-

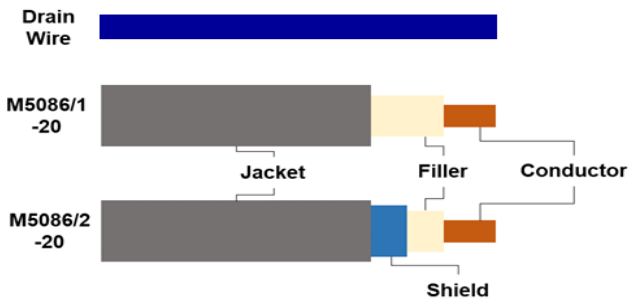

Fig. 2. Components of M5086/1-20, M5086/2-20 cables and drain wire.

B. Cable Test Equipment and Setup

Figure 3 shows the cable bundle test setup represented in DO-160 Section 22. The cable bundle test was conducted at the Avionics Technology Center of the Korea Testing Laboratory, as shown in Fig. 4. A high-power winding resistor (HRW 5000WJ-50R PS) was installed for the EUT (Equipment Under Test), and the power supply for supplying power to the EUT was omitted.

The high-power wire-wound resistor had a rated capacity and resistance of 5000 W/50 Ω, making it suitable for an indirect lightning test in which a current of up to 3200 A is instantaneously generated. A high-power wire-wound resistor was installed on a grounded copper table, and the test cable was connected at both ends. The resistor was connected between two ends of the conductor.

The test waveform was generated using the MIG0618SS Generator of the EMC PARTNER AG, which handles the DO-160 test equipment. The generated test waveform is sent to the CN-GI-CI coupling transformer to generate an electromagnetic field around it. The generated electromagnetic field is strongest inside and outside of an energized coupling transformer and spreads over time into the surrounding space. In addition, the electromagnetic field inside the coupling transformer induces a current in the conductor inside the cable bundle passing through it. The magnitude of the induced current/voltage generated in the conductor can be observed in real-time through an oscilloscope connected to the current and voltage probes.

The drain wire was made of copper and aluminum, and both

endpoints were grounded through a copper table. The drain wire is attached to the side of the cable and goes through a coupling transformer together with the cable bundle. In the cable test, the protection performance of the shielding and drain wire was evaluated by monitoring the magnitude of the internal induced current. The cable protection performance of the shield and drain wire was compared for Waveform 3 and Level 3. Moreover, the cable protection performance of the drain wire was evaluated by varying the number of cables to 1, 3, and 5 in Waveform 1. Level 3 was chosen as the test level for Waveform 1 to simulate the situation inside a rotorcraft cockpit, and Level 5 was selected to represent the most severe environment.

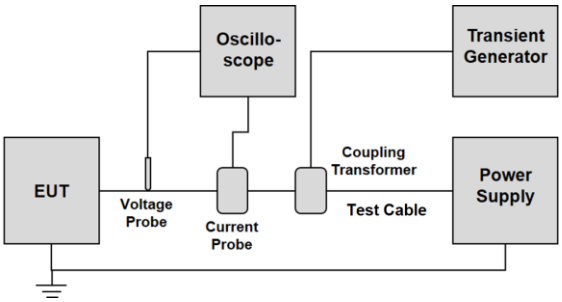

Fig. 3. Cable bundle test setup of DO-160.

C. *Results of the Cable Bundle Test with Protection System*

1) *Cable Test Results for Waveform 3 and Level 3*

The cable bundle test was conducted for Waveform 3 and Level 3 by applying a voltage waveform of 600 V/120 A to one M5086/1-20 cable. Shielding and drain wire were used as the cable protection, and the magnitude of the induced current was measured.

Figure 5 shows the current for the unshielded/shielded cable and the drain wire of copper and aluminum. Table II summarizes the magnitude of the maximum induced current on the cables. An induced current of up to 1470 mA was observed for the unshielded cable. For the shielded cable, a maximum of 570 mA was observed, a reduction of 60.55 % compared to the unshielded cable. An induced current of up to 1360 mA was observed for the cable with an aluminum drain wire. For the cable with a copper drain wire, a maximum of 970 mA was observed. The aluminum and copper drain wires reduced the magnitude of the maximum induced currents by 7.49 % and 34.02 %, respectively, compared to the unshielded cable.

Overall, shielding provided higher cable protection performance than the drain wire, and the copper drain wire with high electrical conductivity showed higher cable protection performance than the aluminum drain wire.

TABLE II
MAXIMUM INDUCED CURRENT ON THE CABLES

Cable Protection System	Maximum Induced Current (mA)
-	1470
Shield	580
Drain Wire – Al	1360
Drain Wire – Cu	970

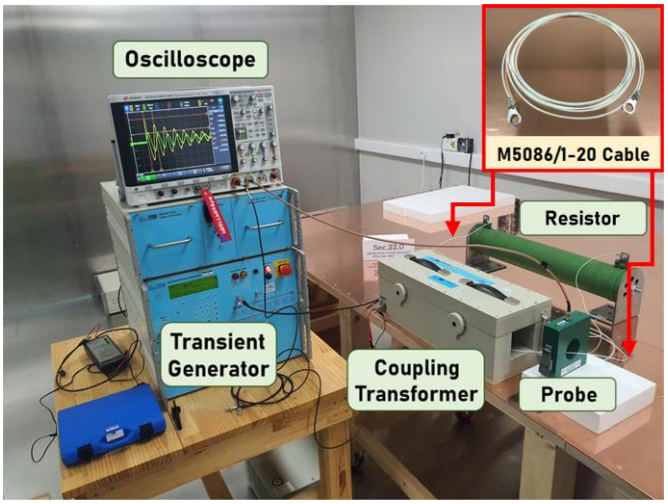

Fig. 4. Test setup for cable bundle test with M5086/1-20 cable.

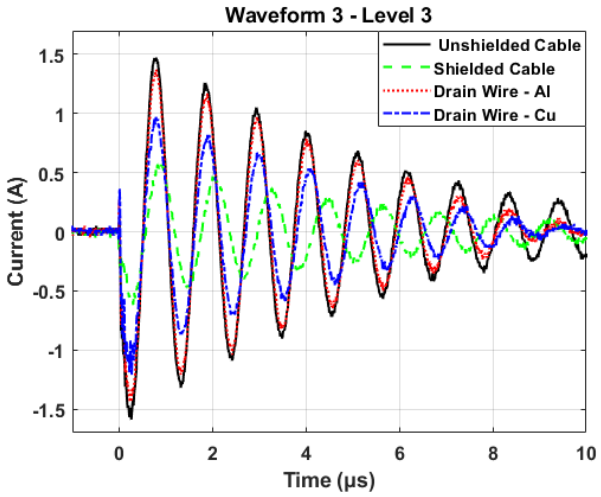

Fig. 5. Test results for Waveform 3 and Level 3.

2) *Cable Test Results for Waveform 1 and Level 3*

Table III shows the cross-sectional views of unshielded cables and cable bundles to which drain wires are applied for each case. The cable bundle test was conducted for Waveform 1 and Level 3 by applying a voltage waveform of 300 V/600 A. The performance of the aluminum and copper drain wires was evaluated by changing the test cables into one, three, and five cables. Table IV summarizes the magnitude of the maximum induced current on the cables with different drain wire materials at Waveform 1 and Level 3. The reduced current ratio indicates the reduction in the current magnitude of cables with drain wire compared to unshielded cables.

Figure 6 compares the induced current of the unshielded cables and the cables with copper and aluminum drain wires. Case 1 represents a test of a cable bundle consisting of one cable and one drain wire. For the unshielded cable, the maximum current magnitude was measured to be 7.49 A. On the other hand, for aluminum and copper drain wires, the maximum current magnitudes in the cable were 4.71 A and 5.07 A, respectively. Aluminum and copper drain wires reduced the maximum induced current magnitude of the unshielded cable (6.41 A) by 37.2 % and 32.4 %, respectively.

Case 2 represents the test of a cable bundle consisting of three

cables and one drain wire. The maximum induced current magnitude of 7.14 A was measured in the unshielded cable. For the aluminum and copper drain wires, the maximum current. Magnitudes in the cable were 4.51 A and 2.21 A, respectively. Aluminum and copper drain wires reduced the maximum induced current magnitude of the unshielded cable (7.14 A) by 36.9 % and 69.1 %, respectively.

Case 3 represents the test of a cable bundle consisting of five cables and one drain wire. Maximums of 6.41 A, 4.08 A, and 1.47 A were measured for the unshielded cable, aluminum, and copper drain wires, respectively. Aluminum and copper drain wires reduced the maximum induced current magnitude of the unshielded cable (6.41 A) by 36.4 % and 77.1 %, respectively.

TABLE III
CROSS SECTIONS OF CABLES USED FOR TESTING

Test Case	Unshielded Cable	Cable with Drain Wire
Case 1, 4		
Case 2, 5		
Case 3, 6		

TABLE IV
MAXIMUM INDUCED CURRENT ON CABLES WITH DIFFERENT DRAIN WIRE MATERIALS AT WAVEFORM 1 AND LEVEL 3

Waveform 1 Level 3		Max Current (A)	Reduction Ratio (%)
Case 1 (One Cable)	-	7.49	-
	Al	4.71	37.2
	Cu	5.07	32.4
Case 2 (Three Cables)	-	7.14	-
	Al	4.51	36.9
	Cu	2.21	69.1
Case 3 (Five Cables)	-	6.41	-
	Al	4.08	36.4
	Cu	1.47	77.1

3) Cable Test Results for Waveform 1 and Level 5

The cable bundle test was conducted for Waveform 1 and Level 5 by applying a voltage waveform of 1600 V/3200 A and for one (case 4), three (case 5), and five (case 6) cables. The level 5 waveform was tested by increasing the raise time so that the peak time exists within 10 μs equal to the level 3 test measurement time. The reason is to prevent fire or electric shock by generating a spark at the grounding point if a high current is injected in a short time. For this reason, the waveforms of test levels 3 and 5 appear different.

Figure 7 compares the induced current of the unshielded cables and the cables with copper and aluminum drain wires. Table V summarizes the magnitudes of the maximum induced current on cables with different drain wire materials at Waveform 1 and Level 5, and the reduced current ratio compared to the unshielded cable.

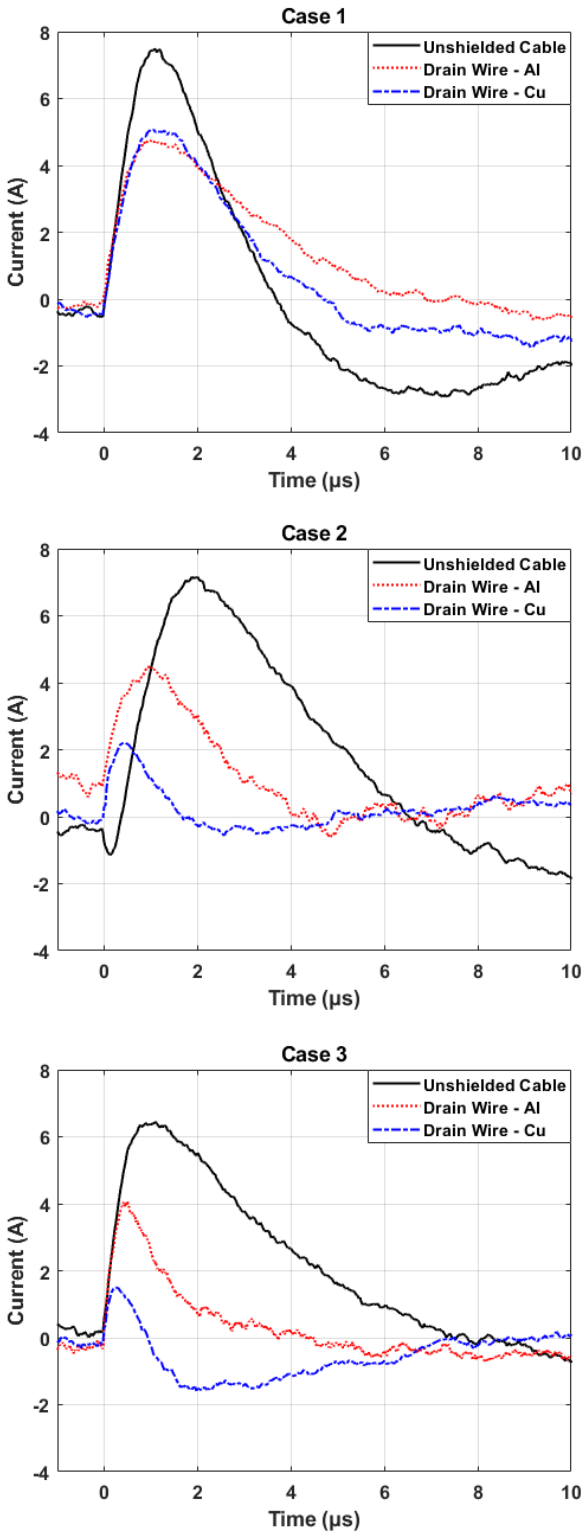

Fig. 6. Comparison of induced current at Waveform 1 and Level 3 condition: (a) case 1 with one cable; (b) case 2 with three cables; (c) case 3 with five cables.

In case 4 with one cable and one drain wire, maximum current magnitudes of 114 A, 79.9 A, and 64.1 A were measured for the unshielded cable, aluminum, and copper drain wires, respectively. Aluminum and copper drain wires reduced the maximum induced current by 29.9 % and 43.8 %.

In case 5 with three cables and one drain wire, maximum current

magnitudes of 76.3 A, 64.2 A, and 43.2 A were measured for the unshielded cable, aluminum, and copper drain wires, respectively. Aluminum and copper drain wires reduced the maximum induced current by 15.9 % and 43.4 %.

In case 6 with five cables and one drain wire, maximum current magnitudes of 34.1 A, 25.4 A, and 24.8 A were measured for the unshielded cable, aluminum, and copper drain wires, respectively. Aluminum and copper drain wires reduced the maximum induced current by 25.6 % and 27.3 %.

TABLE V
MAXIMUM INDUCED CURRENT ON CABLES WITH DIFFERENT DRAIN WIRE MATERIALS AT WAVEFORM 1 AND LEVEL 5

Waveform 1 Level 5		Max Current (A)	Reduction Ratio (%)
Case 4 (One Cable)	-	114	-
	Al	79.9	29.9
	Cu	64.1	43.8
Case 5 (Three Cables)	-	76.3	-
	Al	64.2	15.9
	Cu	43.2	43.4
Case 6 (Five Cables)	-	34.1	-
	Al	25.4	25.6
	Cu	24.8	27.3

D. *Results and Analysis of the Cable Bundle Tests*

In the cable bundle test, the shielding performance was shown to be superior to that of a drain wire for cable protection. For the drain wire, the copper drain wire, with relatively high electrical conductivity, showed better performance than the aluminum drain wire. This is because the electrical conductivity of copper is higher than that of aluminum, so the current flows to the ground plate faster than in aluminum.

On the other hand, in the Level 5 test conducted with a high current, the copper drain wire was expected to perform better than the aluminum drain wire as the number of cables increased. However, as the number of cables increased, contrary to expectations, it was found that the performance of copper and aluminum drain wires became similar. It is believed that as the number of cables surrounding the drain wire increases, the performance of the drain wire is not fully realized compared to the case of a single cable. For this reason, it is expected that the location of the drain wire is also important when applying a drain wire to more than one cable.

Additionally, a low pass filter was applied to the resulting waveform to remove noise from the test site above 5 MHz. However, the graph for the level 5 test contained noise of 5 MHz or less, resulting in the rise time of the copper drain wire appearing higher than that of the aluminum drain wire.

III. COMPUTATIONAL SIMULATION

A. *Computational Analysis Tool*

EMA3D is a three-dimensional Finite Difference Time Domain (FDTD) based electromagnetic field numerical analysis software based on the curl-type Maxwell equations. EMA3D is a specialized software developed to simulate the effect of lightning on aircraft cables [15], [21]. Faraday's electromagnetic induction law and Ampere's law of Maxwell's equations are used to describe the electromagnetic field in space in EMA3D [22]:

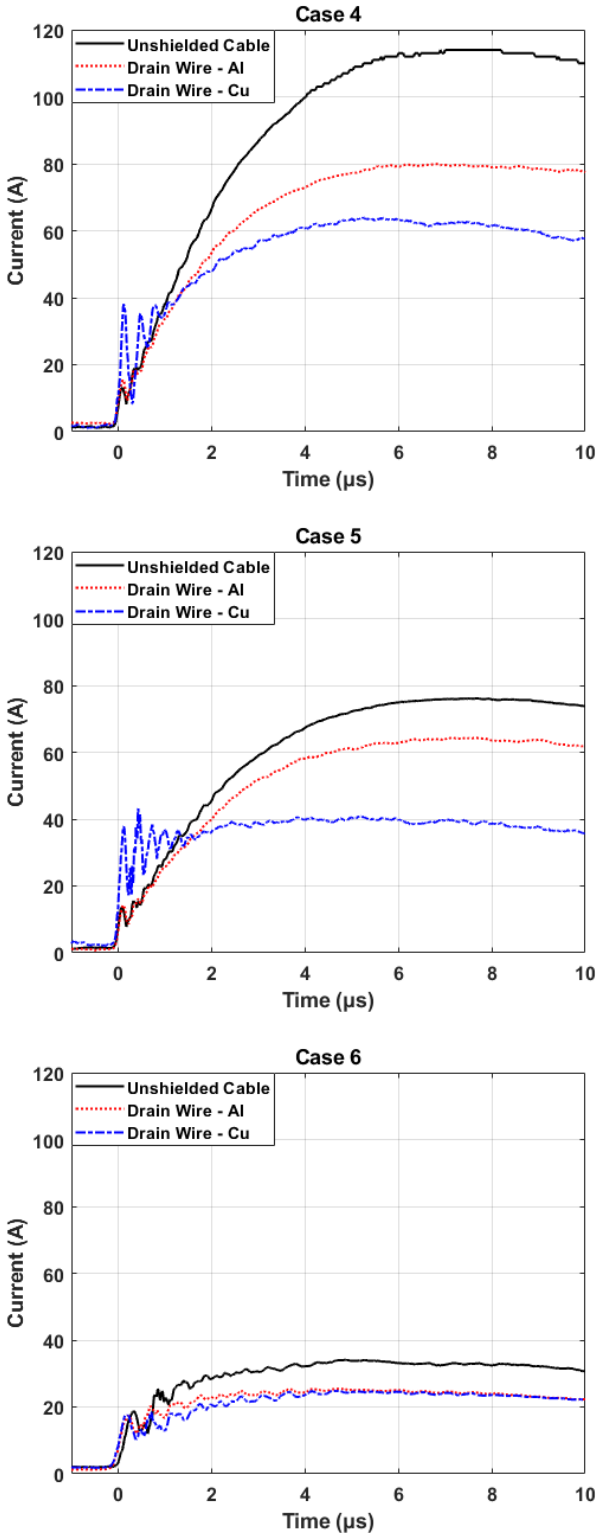

Fig. 7. Comparison of induced current at Waveform 1 and Level 5 condition: (a) case 4 with one cable; (b) case 5 with three cables; (c) case 6 with five cables.

$$\nabla \times \vec{E} = -\mu \frac{\partial \vec{E}}{\partial t} \quad (1)$$

$$\nabla \times \vec{H} = -\varepsilon \frac{\partial \vec{E}}{\partial t} + \sigma \vec{E} + \vec{J} \quad (2)$$

Here E is the electric field, H is the magnetic field, J is the current density, μ is the permeability, ε is the permittivity, and σ is the electrical conductivity.

In addition, another solver, MHARNESS [22], was used, a transmission line solver that enables the user to simulate levels on individual electronic pins at the equipment interface and considers the surrounding cables as inductors and capacitors as current flows in a closed circuit with a potential difference. To analyze the electromagnetic effects, MHARNESS utilizes the staggered nature of TLM analysis and uses transmission line formalism expressed as follows,

$$L\frac{\partial \vec{I}}{\partial t} + R\vec{I} = -\frac{\partial \vec{V}}{\partial x} + \overrightarrow{E_x^{ic}} \quad (3)$$

$$C\frac{\partial \vec{V}}{\partial t} + G\vec{V} = -\frac{\partial \vec{I}}{\partial x} \quad (4)$$

Here I is the cable current, V is the cable voltage, C is the capacitor coefficient, L is the inductance coefficient, R is the resistance, G is the conductivity coefficient, and E is the external electric field.

The FDTD model of EMA3D allows the calculation of the induced current flow on the surface of the analytical model and the associated electromagnetic field. In addition, through the TLM model in MHARNESS, the magnitude of the induced current/voltage generated in the cable can be calculated.

B. Cable Bundle Test Simulation

1) Computational Modeling and Analysis Conditions

Figure 8 shows the computational modeling of the cable bundle test and the cable cross-sections of (a) shielded cable, (b) unshielded cable, and (c) cable with drain wire. The cable bundle was modeled to have a length of 4 m as in the test and to form a closed circuit with both ends connected to a resistor. The drain wire passed through the coupling transformer together with the cable bundle, and both ends are in contact with the wire set to the PEC which is in contact with the boundary. The simulation model for the cable bundle used a total of 10,749,280 cells with a single cell size of 10 mm × 10 mm × 10 mm. In addition, the time step was set to 50 ns, and E-field Low Frequency, a quasi-static analysis that assumes the test object to be in a static state, was selected as the boundary condition having a size of 4140 mm (length) × 780 mm (width) × 720 mm (height). The resistor was modeled to have a length of 600 mm, a diameter of 150 mm, and a resistance of 50 Ω. The coupling transformer was modeled as a perfect electric conductor. The waveform generated by the generator was modeled to generate an induced current in the cable through the coupling transformer. And the current waveform was applied to the injection point of the coupling transformer in the simulation. The transient generator that generates the test waveform is implemented by replacing the generated waveform with an external source that injects it into a coupling transformer.

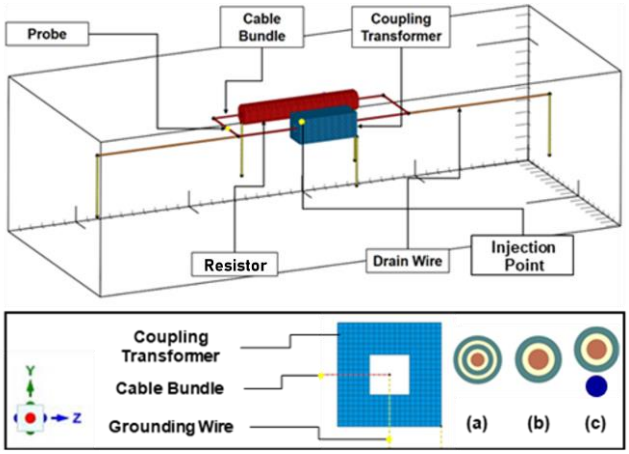

Fig. 8. Computational modeling of the cable bundle test.

2) Comparison of the Cable Bundle Test and Computational Simulation Results

To compare with the cable bundle test results, the case of a cable at Waveform 1 and Level 3 was selected, which can cause a high current instantaneously and greatly affect the internal electronic equipment and cables of the rotorcraft [23], [24].

Figure 9 and Table VI compare the test data and computed results. The maximum induced current magnitudes of the unshielded cable were found to be 7.49 A and 7.44 A in the test and simulation, respectively. On the other hand, when aluminum drain wire was used, it was found to be 4.71 A and 5.06 A, respectively. When copper drain wire was used, it was found to be 5.07 A and 5.08 A, respectively.

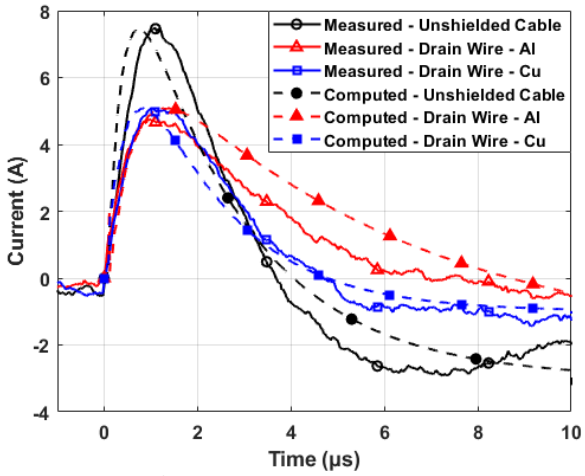

Fig. 9. Comparison of the teat data and computational simulation results.

TABLE VI
RESULT OF THE TEST AND COMPUTATIONAL SIMULATION

Waveform 1 Cable No. 1	Level 3		
	N/A	Al	Cu
Measured (A)	7.49	4.71	5.07
Computed (A)	7.44	5.06	5.08

The computational simulation results were found to be very close to the maximum current value from the cable test. In addition, the results of the computational simulation showed a trend very similar to the cable test results for the change of current with time. Overall, the simulation results were in excellent agreement with those of the test, especially in the case of unshielded and copper drain wire, confirming the high accuracy of the computational simulation using EMA3D and MHARNESS.

C. Computational Simulation for EC-155B

A computational simulation of the rotorcraft was performed to investigate whether the cable protection system (shielding and drain wires) considered in this study could protect the cables inside the rotorcraft.

Lightning current flows into the rotorcraft through the PEC line connected to the blade tip and the boundary, and the electromagnetic field generated through the fuselage causes an induced current in the inner cable. The coupling mechanism of the rotorcraft cable and lightning strike is as follows.

First, after the rotorcraft is struck by lightning, a lightning current flows on the surface of the rotorcraft. The current flowing through the surface generates a magnetic field inside the rotorcraft according to Ampere's law. The generated magnetic field again generates an induced current in the inner cable according to Faraday's law. Through this mechanism, an induced current is generated in the inner cable of the rotorcraft that is struck by lightning. And the induced current generated in the cable can cause disturbance and interference in the signal between the avionics equipment, so a protection system is required to prevent it.

1) Computational Model of EC-155B and Analysis Conditions

The EC-155B is a civilian rotorcraft manufactured by Airbus Helicopters, with a length of 14.3 m, a height of 4.35 m, and a wing diameter of 12.6 m. The surface of the rotorcraft was modeled as carbon-reinforced fiber (CFRP) with an electrical conductivity of 35,000 S/m. On the other hand, the windshield was modeled as polycarbonate with an electrical conductivity of 0 S/m.

A total of 24,826,276 cells with a single cell size of 30 mm × 30 mm × 30 mm were used in the simulation. The time step was set as 100 ns. MUR 1 of H-Fields, which absorbs signals generated from rotorcraft without being reflected at the boundary, was used as the outer boundary condition. The computational model of the EC-155B is shown in Fig. 10.

For the current waveform, the Component A waveform with a maximum of 200 kA classified as Zone 1A in SAE ARP 5414B was injected at the initial attachment point of the lightning [23], [24]. The end of the entry wire is processed to be in contact with the boundary. A computer simulation was conducted for a case in which lightning was attached to the tip of the main blade and released through the nose, which is a typical lightning strike test case for a rotary-wing aircraft [25].

The internal cable harness of the rotorcraft was modeled to connect the cockpit, engine, landing gear, and tail boom as shown in Figure 10. The cable harness was grounded to the rotorcraft surface at the tail boom and the magnitude of the induced current was measured by installing a probe in the cockpit. Shielding and drain wires were used as a cable protection system as shown in Fig. 10. The drain wire was next to the cable bundle and was grounded through the cockpit and tail boom.

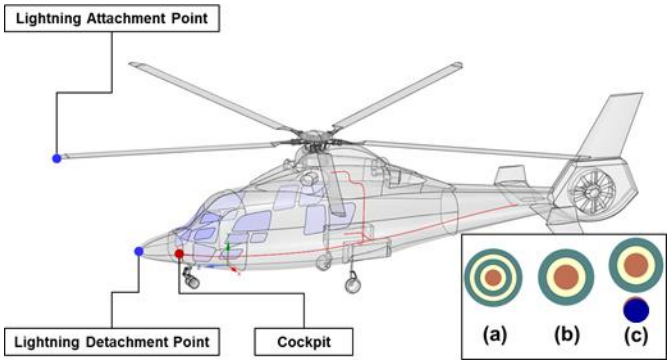

Fig. 10. Computational model of cable harness within EC-155B and cross-section of (a) shielded cable; (b) unshielded cable; and (c) cable with drain wire.

2) Computational Simulation Results for EC-155B

Figure 11 shows the surface current contours when the EC-155B was struck by lightning. Because the surface current density of a rotorcraft body struck by lightning is high around the cockpit, a suitable lightning protection system must be applied to the avionics and cables inside the cockpit.

Figure 12 and Table VII show the waveforms and the magnitude of the maximum induced current when shielding and drain wires were applied to the internal cables of the rotorcraft. When the rotorcraft was struck by lightning, an induced current of up to 195.4 A was generated in the unshielded cable. On the other hand, maximum current magnitudes of 73.0 A, 159.5 A, and 120.6 A were predicted for shielding, aluminum, and copper drain wires, respectively, which are equivalent to current reduction ratios of 62.6 %, 18.4 %, and 38.3 %.

Through the present simulation, it was found that the shielding and drain wires were effective at reducing the maximum induced current generated in the cables inside the rotorcraft. Although the shielding showed the highest protection performance, the copper drain wire was also found to be quite effective.

Fig. 11. Contour plot of the current density on the EC-155B surface.

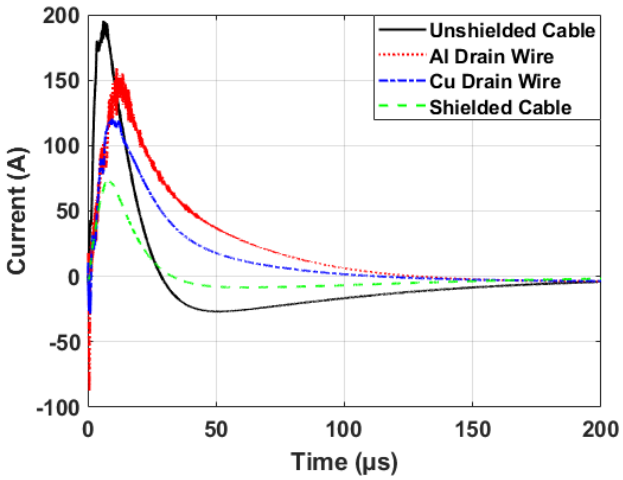

Fig. 12. Computational results of induced currents in unshielded cable, shielded cable, and cable with drain wire.

TABLE VII
RESULTS OF MAXIMUM INDUCED CURRENT AND CURRENT RATIO OF CABLE BUNDLE WITH PROTECTION SYSTEM

	N/A	Shielding	Al Drain Wire	Cu Drain Wire
Max Induced Current (A)	195.4	73.0	159.5	120.6
Reduction Ratio (%)	-	62.6	18.4	38.3

IV. CONCLUSIONS

In this study, shielding and drain wire were considered as methods to protect the cable bundle inside the aircraft from lightning strikes. In the cable bundle test, the shielding generally provided better cable protection than the drain wire. In addition, the copper drain wire performed better than the aluminum drain wire, which has relatively lower electrical conductivity. However, as the number of cables increased, it was found that the performance difference between copper and aluminum drain wires was significantly reduced. It is believed that as the number of cables surrounding the drain wire increases, the performance of the drain wire is not fully realized compared to the case with a single cable.

Next, the computational simulation results obtained using EMA3D and MHARNESS were compared with the cable bundle test results. Overall, the simulation results were in excellent agreement with those from the test, especially in the case of the unshielded and copper drain wire, confirming the high accuracy of the computational simulation. Finally, a computational simulation was performed to examine whether the shielding and drain wires provided a protective effect to the cables inside the actual rotorcraft. The rotorcraft EC-155B and its internal cable harness were modeled for the computational simulation. It was found that the shielding and drain wires were effective at reducing the maximum induced current generated in the cables inside the rotorcraft. Although the shielding showed the highest protection performance, the copper drain wire was also found to be quite effective.

When shielding and drain wire are used, it will inevitably increase the weight of the cable and entail a weight penalty when applied to rotorcraft. Although not covered in this study, it will be necessary to reduce the weight penalty by combining shielding and drain wires or by optimizing the weight of each method for the lightning indirect environment inside the rotorcraft. Also, it will be an interesting research topic to check the maximum induced current change values of the shielding and drain wires confirmed in this study in the frequency domain. We hope to report the results of research on these topics in the future.

REFERENCES

[1] M. Apra, M. D'Amore, K. Gigliotti, M. S. Sarto, and V. Volpi, "Lightning indirect effects certification of a transport aircraft by numerical simulation," *IEEE Transactions on Electromagnetic Compatibility*, vol. 50, no. 3, pp. 513–523, Aug. 2008.

[2] D. Prost, F. Issac, T. Volpert, W. Quenum, and J. Parmantier, "Lightning-Induced current simulation using RL equivalent circuit: application to an aircraft subsystem design," *IEEE Transactions on Electromagnetic Compatibility*, vol. 55, no. 2, pp. 378–384, Apr. 2013.

[3] M. D'Amore, M. S. Sarto, and A. Scarlatti, "Modeling of magnetic-field coupling with cable bundle harnesses," *IEEE Transactions on Electromagnetic Compatibility*, vol. 45, no. 3, pp. 520-530, Aug. 2003.

[4] G. G. Gutierrez, D. M. Romero, M. R. Cabello, E. Pascual-Gil, L. D. Angulo, D. G. Gomez, and S. G. Garcia, "On the design of aircraft electrical structure networks," *IEEE Transactions on Electromagnetic Compatibility*, vol. 58, no. 2, pp. 401–408, Apr. 2016.

[5] E. Perrin, C. Guiffaut, A. Reineix, and F. Tristant, "Using a design-of-experiment technique to consider the wire harness load impedances in the FDTD model of an aircraft struck by lightning," *IEEE Transactions on Electromagnetic Compatibility*, vol. 55, no. 4, pp. 747–753, Aug. 2013.

[6] M. H. Vogel, "Effect of lightning and high-intensity radiated fields on cables in aircraft," *IEEE Transactions on Electromagnetic Compatibility*, vol. 3, no. 2, pp. 56–61, Feb. 2014.

[7] J. J. Kim, S. T. Baek, D. G. Song, and R. S. Myong, "Computational simulation of lightning strike on aircraft and design of lightning protection system," *Journal of the Korean Society for Aeronautical & Space Sciences*, vol. 44, no. 12, pp. 1071-1086, Nov. 2016.

[8] Y. S. Kang, S. W. Park, J. S. Roh, and R. S. Myong, "Computational investigation of effects of expanded metal foils on the lightning protection performance of a composite rotor blade," International Journal of Aeronautical and Space Sciences, vol. 22, no. 1, pp. 203-221, Feb. 2021.

[9] Aerossureance, "When Screens Go Blank: NTSB on a 787 Display Loss After a Lightning Strike," May. 13, 2018. [Online]. Available: http://aerossurance.com/safetymanagement/ntsb-787-lightning-strike/#respond

[10] Flight Safety Foundation, "SU95, Moscow Sheremetyevo Russia, 2019," Jan. 2, 2020. [Online]. Available: https://skybrary.aero/accidents-and-incidents/su95-moscow-sheremetyevo-russia-2019, Sheremetyevo_Russia,_2019

[11] Advisory Circular (AC) 20-136C, *Aircraft Electrical and Electronic System Lightning Protection*, Sep. 2011.

[12] SAE Aerospace Recommended Practice (ARP) 5415B, *User's Manual for Certification of Aircraft Electrical/Electronic Systems for the Indirect Effects of Lightning*, Mar. 2020.

[13] M. Zhang and Z. Huang, "Transient current burst analysis induced in cable harness due to direct lightning strike on aircraft," Presented at the 2010 Asia-Pacific *International Symposium on Electromagnetic Compatibility*, Bejing, China, pp. 1197–1200, Apr. 2010.

[14] J. P. Parmantier, F. Issac, and V. Gobin, "Indirect Effects of Lightning on Aircraft and Rotorcraft," *Aerospace Lab*, Issue 5, AL05-10, Dec. 2012.

[15] D. Lalonde, J. Kitaygorsky, W. Tse, S. Brault, J. Kohler, and C. Weber, "Computational Electromagnetic Modeling and Experimental Validation of Fuel Tank Lightning Currents for a Transport Category Aircraft," *Presented at the International Conference on Lightning and Static Electricity (ICOLSE)*, Toulouse, France, pp. 115-119, Sep. 2015.

[16] L. Huang, C. Gao, F. Guo, and C. Sun, "Lightning indirect effects on helicopter: numerical simulation and experiment validation," *IEEE*

Transactions on Electromagnetic Compatibility, vol. 59, no. 4, pp. 1171–1179, Aug. 2017.
[17] S. M. Wang, X. N. Chen, F. Guo, and L. Y. Huang, "Lightning Indirect Effects on UH-1H Helicopter: Numerical Simulation Analysis and EM Shielding," *Presented at the 2017 IEEE 5th International Symposium on Electromagnetic Compatibility*, Bejing, China, pp. 1-4, Oct. 2017.
[18] T. He, and B. Kuhlman, "Investigation of Test Methods for DO-160 Qualification Tests," 2003 *IEEE Symposium on Electromagnetic Compatibility Symposium Record*, vol. 1, pp. 120-123, Aug. 2003.
[19] K. Filik, S. Hajder, and G. Masłowski, "Multi-stroke lightning interaction with wiring harness: experimental tests and modelling," *Energies*, vol. 14, no. 8, p. 2106, Apr. 2021.
[20] Radio Technical Commission for Aeronautics (RTCA) DO-160, *Environmental Conditions and Test Procedures for Airborne Equipment Section 22–Lightning Induced Transient Susceptibility*, Dec. 2010.
[21] C. Weber, D. Lalonde, W. Tse, S. Brault, F. Ahmad, and J. Kiaygorsky, "Lightning response of a composite wing test box: a validation of simulation results," *Presented at the 2015 Int. Conf. on Lightning and Static Electricity*, Toulouse, France, Sep. 2015.
[22] Electro Magnetic Applications Inc., "EMA3D (Version 4.0) MHarness User Manual," 2014.
[23] SAE Aerospace Recommended Practice (ARP) 5412B, *Aircraft Lightning Environment and Related Test Waveforms*, Jan. 2013.
[24] SAE Aerospace Recommended Practice (ARP) 5414B, *Aircraft Lightning Zoning*, Dec. 2018.
[25] SAE Aerospace Recommended Practice (ARP) 5416A, *Aircraft Lightning Test Methods*, Jan. 2013.

Jaehyeon Jo (M'96) received a B.S. degree in aerospace engineering from Gyeongsang National University, Jinju, the Republic of Korea in 2020. He is currently a graduate student at Gyeongsang National University.

His current research interests include rotorcraft, airworthiness certification, lightning, and aircraft EMC & HIRF.

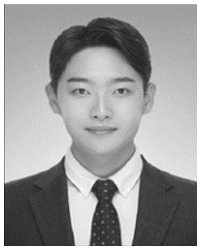

Yungon Kim (M'95) received a B.S. degree in aerospace engineering from Gyeongsang National University, Jinju, the Republic of Korea in 2020. He is currently with Korea Testing Laboratory.

His current research interests include rotorcraft, airworthiness certification, lightning, and aircraft EMC & HIRF.

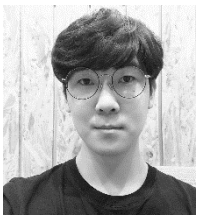

Donghyeon Kim (M'96) received a B.S. degree in aerospace engineering from Gyeongsang National University, Jinju, the Republic of Korea in 2021. He is currently a graduate student at Gyeongsang National University.

His current research interests include rotorcraft, airworthiness certification, lightning, and aircraft EMC & HIRF.

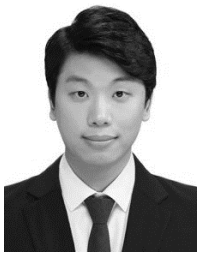

Hakjin Lee (M'89) received a B.S. degree in aerospace engineering from Korea Aerospace University, Seoul, the Republic of Korea in 2012. He received M.S. and Ph.D. degrees in aerospace engineering from the Korea Advanced Institute of Science and Technology, Daejeon, the Republic of Korea in 2014 and 2019, respectively.

Since 2020, he has been working as an assistant professor at Gyeongsang National University, Jinju, the Republic of Korea. He has authored or co-authored 10 papers in journals. His current research interests include rotorcraft, urban air mobility, drones, and computational optimization.

Rho Shin Myong (M'64) received B.S. and M.S. degrees in aeronautical engineering from Seoul National University, Seoul, the Republic of Korea in 1987 and 1989, respectively. He received a Ph.D. degree in aerospace engineering from the University of Michigan, Ann Arbor, USA in 1996.

From 1997 to 1999, he worked as a National Research Council Research Associate at the Space Data and Computing Division of NASA Goddard Space Flight Center, Greenbelt, USA. Since 1999, he has been a professor at Gyeongsang National University, Jinju, the Republic of Korea. In 2017, he became the founding director of the Engineering Research Center for Aircraft Core Technology. He has authored or co-authored more than 140 journal articles. His current research interests include aircraft aerodynamic analysis and design, rarefied gas dynamics, hypersonics, kinetic theory, conservation laws, computational fluid dynamics and heat transfer, computational magnetohydrodynamics, computational electromagnetics, aircraft icing and lightning, and RF and IR low observability.

Prof. Myong is the chair of the 32nd International Symposium on Rarefied Gas Dynamics to be held in Seoul, the Republic of Korea from July 4 to 8, 2022. He is the president of the Korean Society for Computational Fluids Engineering. He is also the associate editor of the International Journal of Computational Fluid Dynamics (Taylor & Francis) and Advances in Aerodynamics (Springer Open). He is an associate fellow of the American Institute of Aeronautics and Astronautics (AIAA) and a member of the American Physical Society (APS) and the Institute of Electrical and Electronics Engineers (IEEE). In recognition of his contribution to the promotion and development of the Korean aerospace industry, he was awarded the 'Korea Aerospace Industries (KAI)-KSAS Aerospace Achievement Award' in 2021, the most prestigious award of the Korean Society for Aeronautical and Space Sciences (KSAS).